

Low-energy excitations in $\text{La}_{1.2}\text{Sr}_{1.8}\text{Mn}_2\text{O}_7$ investigated by ellipsometry

O. Ripeka Mercier,^{1,*} R. G. Buckley,² H. J. Trodahl,¹ C. Bernhard,³ and G. Balakrishnan⁴
¹*MacDiarmid Institute for Advanced Materials and Nanotechnology, Victoria University of Wellington,
P.O. Box 600, Wellington, New Zealand*

²*Industrial Research Limited, P.O. Box 31310, Lower Hutt, New Zealand*

³*Max-Planck Institut für Festkörperforschung, Heisenbergestrasse 1, Stuttgart, Germany*

⁴*Department of Physics, University of Warwick, Coventry CV47AL, United Kingdom*

(Received 17 June 2005; revised manuscript received 3 November 2005; published 29 December 2005)

The low-energy excitations of the bilayered manganite $\text{La}_{1.2}\text{Sr}_{1.8}\text{Mn}_2\text{O}_7$ have been explored by spectral ellipsometry from two faces of a single crystal over the range from 0.006 to 0.6 eV. This compound is a paramagnetic insulator at ambient temperature, with a transition to a ferromagnetic metal below a Curie temperature (T_c) of 125 K. Both the *ab*-plane and *c*-axis temperature-dependent conductivities have been determined. Essentially no temperature-dependent behavior is observed above T_c although below T_c both the phonon and electronic contributions are strongly temperature sensitive. The highest-frequency phonons, especially those involving Mn-O bond stretching, split and show frequency changes consistent with structural results in the literature, and furthermore there is clear evidence of an increase in electron-phonon coupling at and below T_c . We interpret the temperature-dependent electronic spectral contribution in the light of recent calculations that indicate that a mixed phase exists in the doped manganites below T_c , with coexisting regions of an itinerant large-polaron phase and a localized small-polaron phase.

DOI: [10.1103/PhysRevB.72.214437](https://doi.org/10.1103/PhysRevB.72.214437)

PACS number(s): 75.47.Lx, 71.38.-k, 78.20.Ci, 78.30.-j

I. INTRODUCTION

Despite a decade of intensive study the colossal magnetoresistance (CMR) manganites are poorly understood.¹ The conventional picture for the CMR effect is based on the double exchange mechanism proposed more than 50 years ago by Zener.² Within this description the hopping conduction between spin-polarized Mn ions is permitted only if their spins are parallel, so that only in an appropriately doped and ferromagnetic state can charge flow throughout the material. It has been recognized for some years that this model is an inadequate explanation of the coincident ferromagnetic-paramagnetic and metal-insulator (FM-PI) transitions which drive the CMR phenomenon.^{3,4} Although a full description has not been arrived at, recent experimental and theoretical work indicates that the orbital, charge, spin, and lattice degrees of freedom are strongly coupled.¹

The most thoroughly studied CMR materials are the pseudocubic doped rare-earth manganites, $(\text{RE}_{1-x}\text{AE}_x)\text{MnO}_3$. A series of compounds can be derived through partial substitution of the rare earth (RE) ion by an alkaline earth (AE) in the insulating paramagnetic parent compound ($x=0$). The parent compound is known to undergo a cooperative Jahn-Teller (JT) distortion, accompanying a structural transition below 720 K, indicating significant electron-phonon coupling.⁵ The transition to the CMR state, which is coincident with the magnetic/transport transition, depends on the AE concentration.^{1,6,7} The conductivity both above and below the transition is characterized most naturally within a polaron picture, with small- or large-polarons contributing in various temperature and doping regimes.⁸⁻¹⁰ Recent evidence suggests that near and possibly below the transition there exist phase-separated small- and large-polaron regions.¹¹⁻¹³

The pseudocubic manganites, discussed above, are an end member of a Ruddelsden-Popper series, $(\text{RE}_{1-x}\text{AE}_x)_{n+1}\text{Mn}_n\text{O}_{3n+1}$ ($n=1, 2, \dots, \infty$).¹⁴⁻¹⁷ In the $n=2$ layered manganites, each sheet of double-stacked MnO_6 octahedra is sandwiched by insulating rocksalt layers consisting of the rare- and alkaline-earth atoms. These so-called double-layer systems show a strongly two-dimensional conductivity; a much weaker and possible purely incoherent conductivity is measured perpendicular to the MnO_2 sheets. Although some members of the Ruddelsden-Popper manganites are known to undergo phase transitions, controlled by the valence state of the Mn ions, they have been much less thoroughly investigated.¹⁸

One of the most revealing probes of the unusual conduction states in these materials is the conductivity at frequencies that correspond to specific excitations within the charge carriers.^{12,13,19-28} There have been a few earlier determinations of the optical conductivity in the double-layer $\text{La}_{1.2}\text{Sr}_{1.8}\text{Mn}_2\text{O}_7$, although to our knowledge most are based on reflectivity measurements;²⁵⁻²⁸ the exception²⁹ does not extend to the low-energy spectral region probed in the work presented here. Within those studies one finds a number of features familiar from studies of the pseudocubic CMR manganites, including the formation of a polaron band near 1 eV and the appearance of a Drude-like feature that develops as the materials enter the FM phase at low temperature. A question that arises with most of these data sets is that a Kramers-Kronig (KK) analysis requires an extrapolation of the reflectance toward zero frequency, compromising the reliability of the derived optical conductivity in the most important low-energy range of the reflectivity measurements. In this paper we report an ellipsometric study of the *ab*-plane and *c*-axis conductivities at energies from 0.006 to 0.6 eV, measurements that avoid the necessity to extrapolate data outside the measured range.

II. EXPERIMENTAL DETAILS

The crystal used in the study was prepared by a floating zone method as described in an earlier publication.³⁰ Magnetization measurements using a vibrating sample magnetometer confirmed the expected FM transition at a Curie temperature (T_c) of 125 K. Spectral ellipsometry was performed both on a cleaved *ab*-plane surface and on an *ac* plane that was wet polished using Al_2O_3 grains to 1 μm . Oblique incidence ellipsometry from the *ab*-plane was performed using a home-built ellipsometer in combination with a commercial Bruker 113 V Fourier transform interferometer (FTIR) at the Max-Planck-Institut für Festkörperforschung in Stuttgart. The angle of incidence was set at 80° with an angular spread of less than 3° . The ellipsometry measurements from the small (2×3 mm) *ac* surface were performed at the high brilliance source at the U4IR beamline of the National Synchrotron Light Source in Brookhaven National Laboratory. Here we used a home-built ellipsometer in combination with a commercial Nicolet Magna FTIR spectrometer.^{31,32} The angle of incidence was 75° with an angular spread of less than 1.2° . Ellipsometry data from these two faces were then used to extract the *ab*-plane and *c*-axis conductivities, via a numerical decoupling procedure, for energies between 0.006 and 0.6 eV. For temperature-dependent measurements, the sample was placed in a flow-through liquid helium cryostat with diamond windows, enabling spectra to be measured from room temperature down to 10 K.

The inversion of the Fresnel equations from the measured ellipsometric reflection coefficients yields the so-called pseudodielectric function for the measured face. For an optically isotropic material this returns the dielectric function directly. However, if the sample is optically anisotropic, the pseudodielectric function consists of a nontrivial combination of *a*-, *b*-, and *c*-axis dielectric functions. For our uniaxially anisotropic samples, the pseudodielectric functions measured on the *ab* and *ac* planes were decoupled to determine the in-plane and out-of-plane responses with an analysis based on a procedure suggested by Azzam and Bashara.³³ The absence of temperature-dependent *ac*-plane data at energies above 0.087 eV was handled by using the ambient-temperature *c*-axis conductivity at all temperatures. Previous reflectivity measurements justify the procedure, for they confirm the absence of any strong *c*-axis temperature-dependence above the phonon energies.²⁷

The uncertainty in the spectral conductivity is 3% for most of the energy range measured. However, for a small range of energies between 0.07 and 0.1 eV, the uncertainty rises to over 10% due to the sensitivity of the decoupling process to rapid changes in each of the *ac* and *ab* spectra at these energies.

III. RESULTS

Displayed in Fig. 1 is the real part of the *ab*-plane (in-plane) and *c*-axis (out-of-plane) conductivities. The *ab*-plane spectra display phonon modes and a significant electronic background, both of which exhibit considerable temperature dependence that will be discussed below. In contrast the

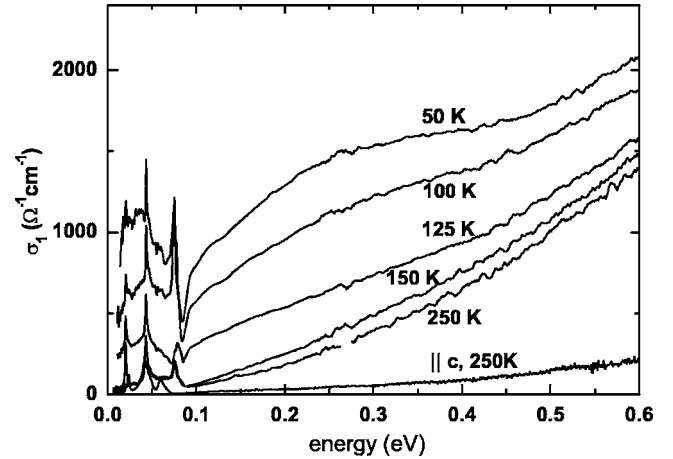


FIG. 1. Energy-dependant *ab*-plane and *c*-axis conductivities. Data at only a selection of temperatures are displayed.

c-axis conductivity (250 K only) exhibits four phonon peaks at low energy, with a very low conductivity background rising with frequency through the mid-IR.

As mentioned above the *ab*-plane spectra are striking in their temperature-induced changes across the entire energy range. The mid-IR 250 K conductivity rises steeply from essentially zero (except for phonon absorption) just below 0.1 eV. Earlier optical measurements have established that this is the low energy side of a broad polaron absorption feature centered at ~ 1 eV which increases in spectral weight and moves to lower energy with decreasing temperature.^{8,9,26–28,34} Interestingly the present data show an additional temperature-dependent feature centered at 250 meV superimposed upon the rising low energy tail of the polaron band, first evident in the 125 K spectrum. This feature grows rapidly in spectral weight with decreasing temperature, at and below T_c , becoming a significant feature at 50 K. The position of the peak displays little temperature dependence.

In addition to the evolving broad feature centered on 250 meV, Fig. 2(a) shows the development of another absorption band below 70 meV again as the material enters the FM phase. At the lowest temperature measure, 10 K, and on the low energy side this band drops sharply towards the measured dc conductivity value. It is important to recall in this connection that the analysis of ellipsometric data does not require an extrapolation to zero energy so these hard to determine, very low energy, conductivity features do not suffer from assumptions contained in the low-energy extrapolation required by a KK analysis. Although the band lies under the phonon modes we believe it to be electronic in origin, a view encouraged by the fact that its low-frequency extrapolation coincides with the measured dc conductivities²⁷ as shown by the symbols along the conductivity axis connected by arrows to the corresponding optical conductivities. The band is distinctly non-Drude-like in its energy dependence, forming instead a broad peak centered at about 37 meV. A similar feature has been reported earlier in $(\text{La}_{0.4}\text{Pr}_{0.6})_{1.2}\text{Sr}_{1.8}\text{Mn}_2\text{O}_7$ and ascribed to disorder-induced localization of the parent compound (zero Pr concentration) carrier excitations.²⁵

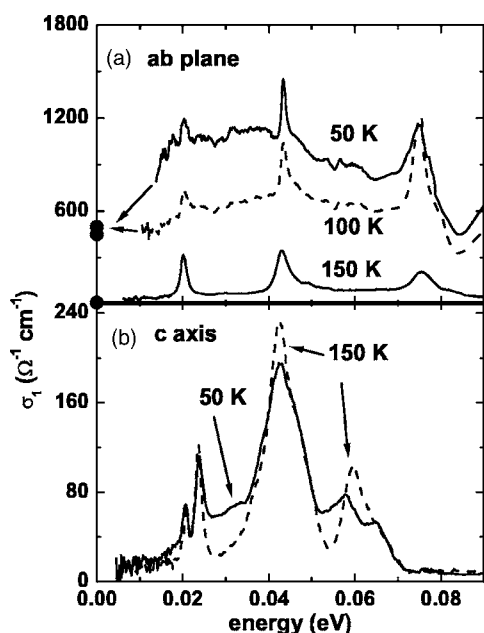


FIG. 2. Spectral conductivity in the low energy region with both phonon and charge carrier contributions. (a) *ab*-plane and (b) *c*-axis conductivity. The *ab*-plane dc conductivities are indicated along the zero-energy axis, and connected to the corresponding spectral data with arrows. Data for only a selection of temperatures are shown.

Figure 2(a) also shows three phonon modes in the *ab*-plane conductivity, fewer than the six E_u zone-center modes predicted by a factor-group analysis.³⁵ At 250 K the three distinct vibrational peaks lie at 20, 43, and 76 meV, on a very weak background as expected for the low dc conductivity measured at these temperatures. There is no measurable temperature dependent behavior of these modes down to 150 K, but at lower temperatures there is evidence for electron-phonon interactions involving the phonons at 43 and 76 meV. The 43 meV phonon narrows significantly below T_c while the 76 meV phonon grows substantially at T_c and below. At 125 K this phonon develops a distinct Fano line shape that continues to evolve with decreasing temperature indicating the onset of a strong interaction between this phonon and an electronic continuum. The temperature dependent behavior of this mode, and in particular the observed loss of spectral weight from the electronic background at high energy (Fig. 1), is dissimilar from the broadening seen in Pr substituted (for La) bilayered manganite.²⁵

Figure 2(b) displays the low-energy (≤ 0.1 eV) out-of-plane conductivity as a function of temperature. At 250 K the spectra are dominated by four vibrational features. Factor group analysis indicates that there are five *c*-axis IR-active A_{2u} modes, so again we observe fewer than the entire set, although the asymmetric feature at 59 meV is likely to be composed of two modes. The spectra show little sensitivity to temperature down to T_c and the modes at 21, 24, and 43 meV display essentially no temperature dependence down to 10 K. Of particular interest is the observation that the high energy asymmetric mode at 59 meV resolves into two distinct modes at T_c .

Between the 24 and 43 meV modes a small increase is observed in the out-of-plane absorption as the temperature is

lowered below T_c . The broad additional absorption in this region bears some similarity to the 37 meV band in the *ab* plane, but it is more than an order of magnitude weaker. It is plausible that the excess absorption in the phonon region is a result of disorder-induced coupling to phonons, though it is then not clear why it is present only in the FM phase. The possibility also exists that there is a weak large-polaron contribution even along the *c* axis; again there is no evidence of it in the dc conductivity.

IV. DISCUSSION

A. Phonon spectra

It was mentioned in the previous section that the highest frequency *ab*-plane and *c*-axis phonons both display a strongly temperature-dependent behavior at and below T_c . These modes involve the oxygen atoms of the MnO_6 octahedra moving against the manganese; they are Mn-O bond stretching modes, and as an aid to understanding the changes with temperature we review the literature as it relates to the configurations of those bonds. Neutron diffraction measurements by Mitchell and co-workers^{15,17} have shown that on traversing T_c to lower temperatures and entering the conducting state there is an increased JT distortion of the MnO_6 octahedra. A rapid change in the unit cell axes over a narrow temperature range near T_c is observed; the *a* axis contracts $\sim 0.16\%$ and the *c*-axis expands 0.06% . These changes in the unit cell are reflected in changes in the bond lengths; the bond to the O(1) oxygen connecting the Mn bilayers is only weakly temperature dependent, the *ab*-plane Mn-O(3) bond lengths decrease rapidly by 0.14% around T_c , and the apical O(2) bond to the Mn atom ionically bonded to the rocksalt layer increases by 0.91% immediately below T_c . The observed resolution of two modes from the asymmetric 59 meV *c*-axis mode, which is dominated by motion of the out-of-plane octahedral oxygen atoms against the manganese [Fig. 2(b)], is consistent with the observed increased distortion of the MnO_6 octahedra at and below T_c . Moreover, the rapid evolution of the *ab*-plane 76 meV mode from a symmetric mode with relatively low oscillator strength to a mode with considerably more strength and a Fano line shape [Fig. 2(a)] indicates again an electron-phonon interaction in this material, facilitated by the JT distortion, that is enhanced at and below T_c .

B. Electronic/polaronic spectra

The most striking feature of the spectra in the FM phase is the rising absorption beginning at T_c and across the entire measurement region of 0.006 to 0.6 eV. A significant fraction of the increased absorption is contained in two bands centered at 37 and 250 meV and, as illustrated in Fig. 3, the two bands grow in perfect concert suggesting a common origin. It is natural to view them as a single polaronic feature that is enhanced by resonance with phonons below 0.085 eV.

It has been demonstrated that the pseudocubic doped rare earth manganites display a significant electron-phonon interaction and it is widely agreed that JT polarons play a

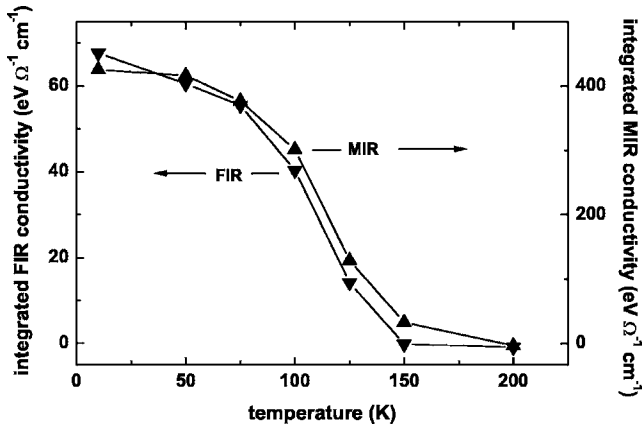


FIG. 3. Comparison of the spectral strengths of the two low-energy *ab*-plane broad peaks. The erect triangles and the right-hand axis represent the strength of the feature centered at 250 meV, integrated from 0.09 to 0.5 eV (MIR), while inverted triangles and the left-hand scale present the integrated strength of the 37 meV peak between 0.01 and 0.09 eV (FIR). Note that the integrations have omitted both the phonon lines and the rising background from the small-polaron tail represented by the 250 K data.

significant role in charge transport. The current IR study clearly shows that this is also true for bilayered $\text{La}_{1.2}\text{Sr}_{1.8}\text{Mn}_2\text{O}_7$. Moreover, Perroni and co-workers¹¹ using a theoretical argument applied to $(\text{La}_{1-x}\text{A}_x)\text{MnO}_3$ at $x=0.3$ suggested that there is a transition, with decreasing temperature, from a paramagnetic insulating phase dominated by small polarons to a ferromagnetic metallic phase dominated by large polarons, passing through a mixed phase with separate regions of high and low charge density. Our data are broadly in agreement with this suggestion. Above T_c $\text{La}_{1.2}\text{Sr}_{1.8}\text{Mn}_2\text{O}_7$ is paramagnetic and as observed in Fig. 1 the IR spectra are dominated by a small polaron centered at about 1 eV having a low energy tail extending to about 0.1 eV. There is no observable electronic contribution below 0.1 eV. Below T_c a population of polarons forms accounting for the growing broad absorption below 0.4 eV and the rising dc conductivity. As discussed above strong electron-phonon coupling is clearly indicated by the Fano line shape of the highest frequency 76 meV mode that develops in the FM phase. Thus the dip at 85 meV separates coupled electron-phonon excitations below that frequency from higher energy small-polaron excitations. It has been impossible to decompose the conductivity into unique small- and large-polaron contributions, especially in the presence of phonons coupled strongly to the electronic excitations. Nonetheless the presence of the two distinct electronic features centered on 250 and 37 meV then suggest that below T_c there is a mixed-phase region, with a FM phase in which delocalized large polarons are the primary current carriers contributing to the low energy excitation spectra, coexisting with the high-temperature-stable paramagnetic phase dominated by small polarons and contributing to the conductivity above 0.5 eV.

A low-energy feature appearing under the phonons, below 0.1 eV, has previously been associated with excitations in the

presence of dynamic orbital disorder, an “orbital liquid.”^{36–39} At first glance the Fano resonance would appear to disagree with the proposal, for it establishes that a strong role is played by phonons rather than orbital excitations. However, the orbital disorder is accompanied in this JT dominated system, with a lattice reorganization, involving just the high-frequency O(Mn) bond stretching vibrational mode that shows the Fano resonance. It has therefore not been possible to discard the orbital-liquid model on the basis of these data.

The broad feature lying under the *c*-axis phonons is superficially similar to the band discussed in the preceding paragraph, but it is a factor of 15 smaller than the in-plane response. It is furthermore not accompanied by a rise at higher frequencies, and we ascribe it to no more than a disorder-induced photon-phonon coupling, which then renders the entire phonon density of modes IR active. It is important to note that this broad and weak band is found only in the FM state, just where various forms of disorder (orbital, structural, phase separation) are indicated by the *ab*-plane spectral conductivity.

V. SUMMARY AND CONCLUSIONS

Spectral ellipsometry has been used to investigate the energy- and temperature-dependent conductivity tensor of the bilayered manganite, $\text{La}_{1.2}\text{Sr}_{1.8}\text{Mn}_2\text{O}_7$, in the spectral range from 0.006 to 0.6 eV. Both the in- and out-of-plane temperature-dependent conductivities have been determined. Very little temperature-dependent behavior is observed in the paramagnetic insulating phase above the Curie temperature but in common with other CMR results there are striking changes across T_c and into the ferromagnetic metallic phase. The strong temperature dependence of especially the *ab*-plane vibrational and electronic spectral conductivities, signals changes to the structure and coupling between the charge and phononic excitations. The changes are particularly strong in the highest-energy *ab*-plane phonon and the electronic contribution at low energy; a broad electronic band is found to grow in the FM phase, extending from the dc limit up to 0.4 eV. Coupling between the band and in-plane phonons leads to changes in the phononic lines, including the development of a clear Fano line shape for the *ab*-plane Mn-O bond stretching excitation. Furthermore, the electronic absorption, which at all temperatures shows evidence of polaronic absorption, is substantially enhanced in the phonon energy region below 0.08 eV upon entering the FM phase. We suggest the enhancement is related to JT disorder-induced electron-phonon coupling across the entire vibrational density of modes as the developing large polarons gain spectral weight at phonon frequencies.

The *c*-axis response similarly shows developments below the Curie temperature, though these changes are not accompanied by an increasing electronic response. In particular the high energy *c*-axis phonon resolves into two clearly defined peaks below T_c . There is, however, a weak rising background in the *c*-axis response, again resembling the phonon density of modes, which confirms the presence of disorder-induced coupling, in this case between phonons and photons.

It is concluded that the temperature-dependent behavior of the phonons indicates an increased electron-phonon coupling at and below T_c consistent with the observed increased lattice distortion upon entering the FM state. In light of the evidence of an increase in electron-phonon coupling we have suggested that the increased *ab*-plane conductivity with decreasing temperature in the FM phase is consistent with recent calculations indicating that with the onset of large polaron formation at T_c there is a development of a mixed phase state consisting of coexisting regions of itinerant large polarons and regions of localized small polarons.

ACKNOWLEDGMENTS

We are very grateful to Todd Holden and Josef Humlicek for their support during the ellipsometry measurements. This study was undertaken in part at the U4IR beamline of the NSLS at Brookhaven and we would also like to acknowledge the technical support of L. Carr and M. Pilling. A. Golnik kindly provided the ellipsometry reduction program. This work was supported by a Royal Society of New Zealand through the Marsden Fund and the International Science and Technology Linkages Fund, a Max-Planck-Institut-FKF Grant, and by the New Zealand Foundation for Research, Science, and Technology.

*Present address: Te Kawa a Māui, Victoria University of Wellington, P.O. Box 600, Wellington, New Zealand. Email address: ocean.mercier@vuw.ac.nz

- ¹M. Imada, A. Fujimori, and Y. Tokura, *Rev. Mod. Phys.* **70**, 1039 (1998).
- ²C. Zener, *Phys. Rev.* **82**, 403 (1951).
- ³A. J. Millis, P. B. Littlewood, and B. I. Shraiman, *Phys. Rev. Lett.* **74**, 5144 (1995).
- ⁴A. E. Pantoja, H. J. Trodahl, A. Fainstein, R. G. Pregliasco, R. G. Buckley, G. Balakrishnan, M. R. Lees, and D. McK. Paul, *Phys. Rev. B* **63**, 132406 (2001).
- ⁵E. Granado, J. A. Sanjurjo, C. Rettori, J. J. Neumeier, and S. B. Oseroff, *Phys. Rev. B* **62**, 11304 (2000).
- ⁶R. von Helmolt, J. Wecker, B. Holzapfel, L. Schultz, and K. Samwer, *Phys. Rev. Lett.* **71**, 2331 (1993).
- ⁷S. Jin, T. H. Tiefel, M. McCormack, R. A. Fastnacht, R. Ramesh, and L. H. Chen, *Science* **264**, 413 (1994).
- ⁸A. J. Millis, R. Mueller, and B. I. Shraiman, *Phys. Rev. B* **54**, 5389 (1996).
- ⁹A. J. Millis, R. Mueller, and B. I. Shraiman, *Phys. Rev. B* **54**, 5405 (1996).
- ¹⁰A. S. Alexandrov and A. M. Bratkovsky, *Phys. Rev. B* **60**, 6215 (1999).
- ¹¹C. A. Perroni, G. De Filippis, V. Cataudella, and G. Iadonisi, *Phys. Rev. B* **64**, 144302 (2001).
- ¹²K. Takenaka, Y. Sawaki, and S. Sugai, *Phys. Rev. B* **60**, 13011 (1999).
- ¹³R. Mathieu, D. Akaoshi, A. Asamitsu, Y. Tomioka, and Y. Tokura, *Phys. Rev. Lett.* **93**, 227202 (2004).
- ¹⁴R. A. M. Ram, P. Ganguly, and C. N. R. Rao, *J. Solid State Chem.* **70**, 82 (1997).
- ¹⁵J. F. Mitchell, D. N. Argyriou, J. D. Jorgensen, D. G. Hinks, C. D. Potter, and S. D. Bader, *Phys. Rev. B* **55**, 63 (1997).
- ¹⁶M. Kubota, H. Fujioka, K. Ohoyama, K. Hirota, Y. Moritomo, H. Yoshizawa, and Y. Endoh, *J. Phys. Chem. Solids* **60**, 1161 (1999).
- ¹⁷C. D. Ling, J. E. Millburn, J. F. Mitchell, D. N. Argyriou, J. Linton, and H. N. Bordallo, *Phys. Rev. B* **62**, 15096 (2000).
- ¹⁸T. Kimura and Y. Tokura, *Annu. Rev. Mater. Sci.* **30**, 451 (2000).
- ¹⁹O. R. Mercier, R. G. Buckley, A. Bittar, H. J. Trodahl, E. M. Haines, J. B. Metson, and Y. Tomioka, *Phys. Rev. B* **64**, 035106 (2001).
- ²⁰K. Takenaka, Y. Sawaki, R. Shiozaki, and S. Sugai, *Phys. Rev. B* **62**, 13864 (2000).
- ²¹K. Takenaka, K. Iida, Y. Sawaki, S. Sugai, Y. Moritomo, and A. Nakamura, *J. Phys. Soc. Jpn.* **68**, 1828 (1999).
- ²²K. Takenaka, R. Shiozaki, and S. Sugai, *Phys. Rev. B* **65**, 184436 (2002).
- ²³Ch. Hartinger, F. Mayr, A. Loidl, and T. Kopp, *Phys. Rev. B* **70**, 134415 (2004).
- ²⁴Ch. Hartinger, F. Mayr, J. Deisenhofer, A. Loidl, and T. Kopp, *Phys. Rev. B* **69**, 100403(R) (2004); Ch. Hartinger, F. Mayr, A. Loidl, and T. Kopp, *ibid.* **71**, 184421 (2005).
- ²⁵J. D. Woodward, J. Choi, J. L. Musfeldt, J. T. Haraldsen, M. Apostu, R. Suryanarayanan, and A. Revcolevschi, *Phys. Rev. B* **69**, 104415 (2004).
- ²⁶T. Ishikawa, T. Kimura, T. Katsufuji, and Y. Tokura, *Phys. Rev. B* **57**, R8079 (1998).
- ²⁷T. Ishikawa, K. Tobe, T. Kimura, T. Katsufuji, and Y. Tokura, *Phys. Rev. B* **62**, 12354 (2000).
- ²⁸H. J. Lee, K. H. Kim, J. W. Jung, T. W. Noh, R. Suryanarayanan, G. Dhalenne, and A. Revcolevschi, *Phys. Rev. B* **62**, 11320 (2000).
- ²⁹J. Kunze, S. Naler, J. Bäckström, M. Rübhausen, and J. F. Mitchell, *Phys. Rev. B* **67**, 134417 (2003).
- ³⁰G. Balakrishnan, M. R. Lees, and D. McK. Paul, *Chem. Mater.* **9**, 1471 (1997).
- ³¹R. W. Henn, C. Bernhard, A. Wittlin, M. Cardona, and S. Uchida, *Thin Solid Films* **313-314**, 643 (1998).
- ³²C. Bernhard, J. Humlicek, and B. Keimer, *Thin Solid Films* **455-456**, 143 (2004).
- ³³R. M. A. Azzam and N. M. Bashara, *Ellipsometry and Polarized Light* (Elsevier, New York, 1977).
- ³⁴M. Cuoco, C. Noce, and A. M. Ole, *Phys. Rev. B* **66**, 094427 (2002).
- ³⁵D. L. Rousseau, R. P. Bauman, and S. P. S. Porto, *J. Raman Spectrosc.* **10**, 253 (1981).
- ³⁶P. Horsch, J. Jakli, and F. Mack, *Phys. Rev. B* **59**, 6217 (1999).
- ³⁷F. Mack and P. Horsch, *Phys. Rev. Lett.* **82**, 3160 (1999).
- ³⁸S. Ishihara, M. Yamanaka, and N. Nagaosa, *Phys. Rev. B* **56**, 686 (1997).
- ³⁹J. Bala, P. Horsch, and F. Mack, *Phys. Rev. B* **69**, 094415 (2004).